



CircRNA_0050486 promotes cell apoptosis and inflammation by targeting *miR-1270* in atherosclerosis

Kai Wang^{1#}, Xiaolong Bai^{2#}, Lili Mei³, Yanping Miao², Feng Jin²

¹Department of Neurosurgery, The Affiliated Hospital of Inner Mongolia Medical University, Hohhot, China; ²Department of Radiology, the Affiliated Hospital of Inner Mongolia Medical University, Hohhot, China; ³Medical School, Kunming University of Science and Technology, Kunming, China

Contributions: (I) Conception and design: F Jin, K Wang; (II) Administrative support: None; (III) Provision of study materials or patients: None; (IV) Collection and assembly of data: XL Bai, LL Mei, YP Miao; (V) Data analysis and interpretation: K Wang, XL Bai, LL Mei, YP Miao; (VI) Manuscript writing: All authors; (VII) Final approval of manuscript: All authors.

[#]These authors contributed equally to this work.

Correspondence to: Feng Jin. Department of Radiology, The Affiliated Hospital of Inner Mongolia Medical University, Hohhot 010050, China. Email: doctorjinfeng@nmgy.com.

Background: Atherosclerosis (AS) is a chronic inflammatory disease that plays a major role in cardiovascular disease. Circular RNAs (circRNAs) are related to the pathogenesis of AS, including the inflammatory response. This study aimed to explore the underlying mechanisms of circRNAs and how they regulate the inflammatory response in AS.

Methods: Analyzed the expression profile of circRNAs in three oxidized low-density lipoprotein (oxLDL) treated macrophage samples and three macrophage control samples using bioinformatics methods. Expression and biological function of circRNA were verified in oxLDL-induced THP-1 macrophages. MiRNAs and target genes of circRNA were predicted by functional enrichment analysis. Expression and function of circRNA target miRNAs were explored in oxLDL-induced THP-1 macrophages. Finally, we predicted and analyzed the function of circRNAs-miRNAs target genes in AS.

Results: We identified nine upregulated circRNAs and found that *circ_0050486* was significantly upregulated in a THP-1 + PMA + oxLDL group compared with a THP-1 + PMA group. Additionally, *circ_0050486* knockdown markedly inhibited IL-6 and TNF- α concentrations and the cell death rates in oxLDL-induced THP-1 macrophages. Furthermore, *circ_0050486* targeted and inhibited *miR-145* and *miR-1270*. Upregulated *miR-1270* markedly inhibited IL-6 and TNF- α levels and the cell death rates in oxLDL-induced THP-1 macrophages. Finally, the target genes of *miR-1270* and *miR-145* were predicted by the miRDB, miRWalk, and Targetscan databases, and a functional analysis network of the target genes was constructed by Cytoscape GlueGO, including the regulation of the immune response and monocyte chemotaxis. The common target genes of *miR-145* and *miR-1270* were established by Cytoscape and included NF1A, among others.

Conclusions: Our study suggested that *circ_0050486* knockdown inhibited inflammation and apoptosis by targeting *miR-1270* in oxLDL-induced THP-1 macrophages. This finding may provide a potential therapeutic target for atherosclerosis.

Keywords: Atherosclerosis (AS); *circ_0050486*; inflammation; apoptosis; *miR-1270*

Submitted Jun 23, 2022. Accepted for publication Aug 17, 2022.

doi: 10.21037/atm-22-3745

View this article at: <https://dx.doi.org/10.21037/atm-22-3745>

Introduction

Atherosclerosis (AS) is a chronic inflammatory disease and remains a major cause of cardiovascular disease (1). Previous studies have reported that the pathogenesis of AS is characterized by endothelial damage, metabolic disorder, inflammatory reactions, foam cell formation, and plaque rupture (2,3). Inflammation contributes to atherosclerotic plaque formation and rupture (4). Furthermore, oxidized low-density lipoprotein (oxLDL) stimulates monocyte recruitment by releasing pro-inflammatory molecules, which induce the differentiation of monocytes into macrophages and promote AS development (5), and induces endothelial cell injury to participate in the pathogenesis of AS (6). Therefore, identifying effective AS biomarkers or therapeutic targets has clinical and theoretical importance.

Circular RNAs (circRNAs) are a special class of non-coding RNA (ncRNA) molecules, which have a closed ring structure without 3'- and 5'-ends compared with linear RNA (7). Studies have shown that circRNAs can act as competing endogenous RNAs (ceRNAs) to decrease the inhibition of miRNAs on their target genes and promote target gene expression in cells (8,9). Mounting evidence confirms the dysregulated expression and biological functions of circRNAs in various diseases, including heart failure, breast cancer, lung cancer, osteosarcoma, and coronary artery disease (10,11). Recent studies have found that circRNAs play a key role in the development and progression of AS (12,13). For example, Zeng *et al.* reported that *circMAP3K5* decreased human coronary artery smooth muscle cells proliferation by targeting the *miR-22-3p/TET2* axis (14). However, the specific details of circRNAs effect on the inflammatory response in AS remain unclear.

In our study, we analyzed the expression profile of circRNAs in three oxLDL-treated macrophage samples and three macrophage control samples using bioinformatics methods. The expression and biological function of *circ_0050486* were verified in oxLDL-induced THP-1 macrophages. Next, the miRNA and target genes of *circ_0050486* were predicted by functional enrichment analysis. Further, the expression and function of *circ_0050486* target miRNAs were explored in oxLDL-induced THP-1 macrophages. Finally, we identified the biological function and mechanism of *circ_0050486* and the targeted miRNAs in AS. We present the following article in accordance with the MDAR reporting checklist (available at <https://atm.amegroups.com/article/view/10.21037/atm-22-3745/rc>).

Methods

Data collection and processing

The study was conducted in accordance with the Declaration of Helsinki (as revised in 2013). We downloaded the GSE107522 dataset from the Gene Expression Omnibus (GEO) database. The GSE107522 dataset included three oxLDL-treated macrophage samples and three macrophage control samples.

Differentially expressed circRNAs (DECs) analysis

After data normalization, we performed a DECs analysis using R software (version 3.24.3, <http://bioconductor.org>) based on $|\log_2 \text{fold change (FC)}| > 1$ and a P value < 0.05 in three macrophage control samples and three oxLDL-treated macrophage samples. A heatmap and volcano plot of the upregulated DECs visualized the results using the “ggplot2” and “pheatmap” R software packages.

Prediction of circRNA-targeted miRNAs

To further demonstrate the potential mechanism of *circ_0050486* in AS, the interacting miRNAs of *circ_0050486* were predicted with CircRNA Interactome (<https://circinteractome.irp.nia.nih.gov/>) (15). The *circ_0050486*-miRNA network was visualized using Cytoscape software (<http://www.cytoscape.org/>).

Predicting the target genes of miRNAs

The *miR-145* and *miR-1270* target prediction databases miRWalk (16), Targetscan, and miRDB (17) were used to predict the target mRNAs of *miR-145* and *miR-1270*. We obtained the common predicted target genes using Perl script based on the three databases. Finally, the common target genes were enriched and visualized using Cytoscape software.

Functional enrichment analysis

ClueGO is a useful plug-in tool in Cytoscape that visualizes the functional ontology and pathway annotation networks of target genes for functional enrichment analysis (18). We used Cytoscape ClueGO for the functional enrichment analysis of the target genes. Through the above steps, we construct the ceRNA network.

Table 1 Specific primers used for the quantitative qRT-PCR analysis

Gene name	Sequence
<i>hsa_circ_0005699</i>	F: GGCATCTTCACACGTCTCAA R: CGGGTACAAGGGGAGGTAAG
<i>hsa_circ_0050486</i>	F: ACTCACATTGCCAAAACCTT R: AAGGGCTTCAGTCACCATGA
<i>hsa_circ_0007478</i>	F: TGCCTACATTCTGCTCACA R: TCCCAAGTACCAAGTGCAT
<i>hsa_circ_0026218</i>	F: CGGCTCTGTGACACCCTTTT R: CCAATCCAGCTGCTTTGACA
<i>hsa_circ_0092327</i>	F: GCAGAGGGTTCAGTGAGGAT R: GCCATCACCTCTCCTCACTT
<i>hsa_circ_0092283</i>	F: AAGGGTTTGGTGGGATCCTG R: CATTTTCCCCTAAGCGCCTG
<i>hsa_circ_0003645</i>	F: CTGCTTCATCACCATCCCCT R: AATCACGGCCAAAGGAAACC
<i>hsa_circ_0064924</i>	F: TTGGCCTCAGCTCTTGAGG R: CATGCACTGTCTTCTGGG
<i>hsa_circ_0008896</i>	F: CGCCCCGATTCTTTTACCG R: TCTTGCTGTTCGCCGATA
<i>miR-1270</i>	F: GGGCTGGAGATATGGAAGA R: CAGTGCCTGTCGTGGAGT
<i>miR-1272</i>	F: GGGGATGATGATGGCAGCAAAT R: CAGTGCCTGTCGTGGAGT
<i>miR-145</i>	F: GGGGTCCAGTCCCAGGA R: CAGTGCCTGTCGTGGAGT
<i>miR-182</i>	F: GGGTGGCAATGGTAGAACT R: CAGTGCCTGTCGTGGAGT
<i>miR-409-3p</i>	F: GGGGAATGTGCTCGGTGA R: CAGTGCCTGTCGTGGAGT
<i>miR-431</i>	F: GGGTGTCTGCAGGCCGT R: CAGTGCCTGTCGTGGAGT
<i>miR-432</i>	F: GGGTCTGGAGTAGGTCAT R: CAGTGCCTGTCGTGGAGT
<i>miR-615-5p</i>	F: GGGGGGGTCCCCGGTGCT R: CAGTGCCTGTCGTGGAGT
<i>miR-620</i>	F: GGGATGGAGATAGATAT R: CAGTGCCTGTCGTGGAGT

qRT-PCR, quantitative real-time reverse transcription polymerase chain reaction.

Cell culture and treatment

The human monocyte cell line THP-1 was obtained from the American Type Culture Collection (ATCC). The THP-1 cells were cultured in RPMI1640 (Gibco, USA) containing 10% fetal bovine serum, 100 U/mL streptomycin, and 100 µg/mL penicillin. The THP-1 cells were cultured in a humidified incubator with 5% CO₂ at 37 °C. When the cells were cultured to 80% confluency, 100 ng/mL Phorbol 12-myristate 13-acetate (PMA) was added to the cells for 72 h to induce differentiation of monocytes (THP-1 cells) to macrophages. The cell model was established by oxLDL. Then, the macrophages were induced with 100 µg/mL oxLDL to form foam cells.

Cell transfection

For cell transfection, plasmids containing short hairpin RNA (shRNA) targeting *circ_0050486* or negative control (NC), mimic-NC, and *miR-1270* mimics (Shanghai Rainbow Co. Ltd., Shanghai, China) were transfected into oxLDL-induced THP1-macrophages using Lipofectamine 2000 (Invitrogen, CA, USA). The cells were cultured for 48 h before subsequent experiments.

Quantitative real-time reverse transcription polymerase chain reaction (qRT-PCR) assay

Total RNA was isolated from the differently treated THP-1 cells using Trizol reagent (Invitrogen, USA). The total RNA was synthesized to cDNA using a miRNA reverse transcription kit (Takara, Japan). The qRT-PCR assay was measured with a cDNA template on an ABI 7500 fast PCR system. GAPDH and U6 were used as the internal reference genes for circRNAs and miRNAs. The relative expressions were analyzed by the 2^{-ΔΔCt} method. The sequence for each primer is shown in *Table 1*.

Enzyme-linked immunosorbent assay (ELISA)

The ELISA kits for interleukin-6 (IL-6) (cat. no. CSB-E04638h) and tumor necrosis factor-alpha (TNF-α) (cat. no. CSB-E04740) were purchased from Wuhan Cusabio Biotechnology Co., Ltd. (Wuhan, Hubei, China). The reagents and samples were prepared according to the manufacturer's instructions. Within 5 minutes of the termination of the reaction, the optical density (OD) of each hole was measured sequentially at a wavelength of 450 nm with an enzyme labeling instrument. Three independent

experiments were conducted.

Cell apoptosis assay

The cell apoptosis rates were determined by flow cytometry assay. Briefly, the differently treated THP-1 cells were collected and washed twice with PBS. Flow cytometry binding buffer (600 μ L) was added to the cells. Then, the cells were stained with Annexin V/FITC (5 μ L) and 5 μ L PI and incubated in the dark for 15 min. The apoptosis rate was detected with a Novocyte flow cytometer (ACEA Biosciences Inc., San Diego, CA, USA).

Dual-luciferase reporter gene assay

The binding sites between *circ_0050486* and *miR-145* or *miR-1270* were predicted by the CircInteractome online database. The correctly sequenced *circ_0050486* WT and *circ_0050486* MUT luciferase reporter plasmids were transfected to the model cells with *miR-145* mimic or *miR-1270* mimic and mimic-NC. Following 48 h transfection, the dual-luciferase reporter assay was used to detect the luciferase activity.

Statistical analysis

SPSS20.0 software was used for the statistical analysis. The collected data are presented as means \pm SD from at least three repeated experiments. One-way analysis of variance (ANOVA) or the Student's *t*-test was used for the between-group comparisons, where a P value <0.05 was considered statistically significant.

Results

Identification of DECs in the oxLDL-treated macrophages

To explore the circRNA function in AS, we analyzed the circRNA expression profiles from the GSE107522 dataset. A total of nine DECs were obtained and are shown in the heatmap (Figure 1A) and volcano plot (Figure 1B). The nine upregulated circRNAs were analyzed with R software using the limma package based on $|\log_2FC| > 1$ and $P < 0.05$ in oxLDL-induced THP-1 macrophages compared with the control group. A qRT-PCR assay was conducted to verify the expression level of the nine DECs in oxLDL THP-1 macrophages. Compared with the THP-1 + PMA group, the mRNA levels of *bas_circ_0050486*, *bas_*

circ_0007478, *bas_circ_0026218*, *bas_circ_0092283*, *bas_circ_003645*, and *bas_circ_0008896* were markedly increased in the THP-1 + PMA + oxLDL group (Figure 1C). Of these, *bas_circ_0050486* had the most significantly increased mRNA level compared with the THP-1 + PMA group. Therefore, we chose *bas_circ_0050486* to explore the function and molecular mechanism of the THP-1 + PMA + oxLDL group.

Knockdown of *circ_0050486* inhibited inflammation and apoptosis in oxLDL-induced THP-1 macrophages

We performed qRT-PCR, ELISA, and flow cytometry assays to investigate the functions of *circ_0050486* in AS. Firstly, we demonstrated the sequence characteristics of *circ_0050486* (Figure 2A). The shRNA-1, shRNA-2, and shRNA-3 of *circ_0050486* were constructed into lentivirus and then transfected into oxLDL-induced THP-1 macrophages. Our results showed that the level of *circ_0050486* was significantly suppressed after *circ_0050486* shRNA1 and shRNA2 transfection, with the shRNA1 *circ_0050486* transfection being the most significant (Figure 2B). Next, IL-6 and TNF- α concentrations were detected by ELISA. The results showed that *circ_0050486* shRNA1 significantly inhibited IL-6 and TNF- α levels in the model cells compared with NC cells (Figure 2C). Furthermore, cell apoptosis was detected by flow cytometry assay, and the results demonstrated that *circ_0050486* shRNA1 suppressed the apoptotic rates (Figure 2D). These results suggested that knockdown of *circ_0050486* repressed the inflammatory response and apoptosis in oxLDL-induced THP-1 macrophages.

Circ_0050486 suppressed inflammation and apoptosis by targeting *miR-1270* in an oxLDL-induced THP-1 macrophage phenotype

To investigate how *circ_0050486* regulated inflammation and apoptosis in AS, we looked for the downstream target genes of *circ_0050486* using the CircRNA Interactome database. As shown in Figure 3A, nine miRNAs were predicted as the potential target miRNAs of *circ_0050486*. The qRT-PCR assay showed that *miR-1270*, *miR-145*, and *miR-182* were negatively correlated with *circ_0050486*. The expression of *miR-1270*, *miR-145*, and *miR-182* were significantly decreased in the model group compared with the control group, and knockdown of *circ_0050486* markedly increased the expression of *miR-1270*, *miR-*

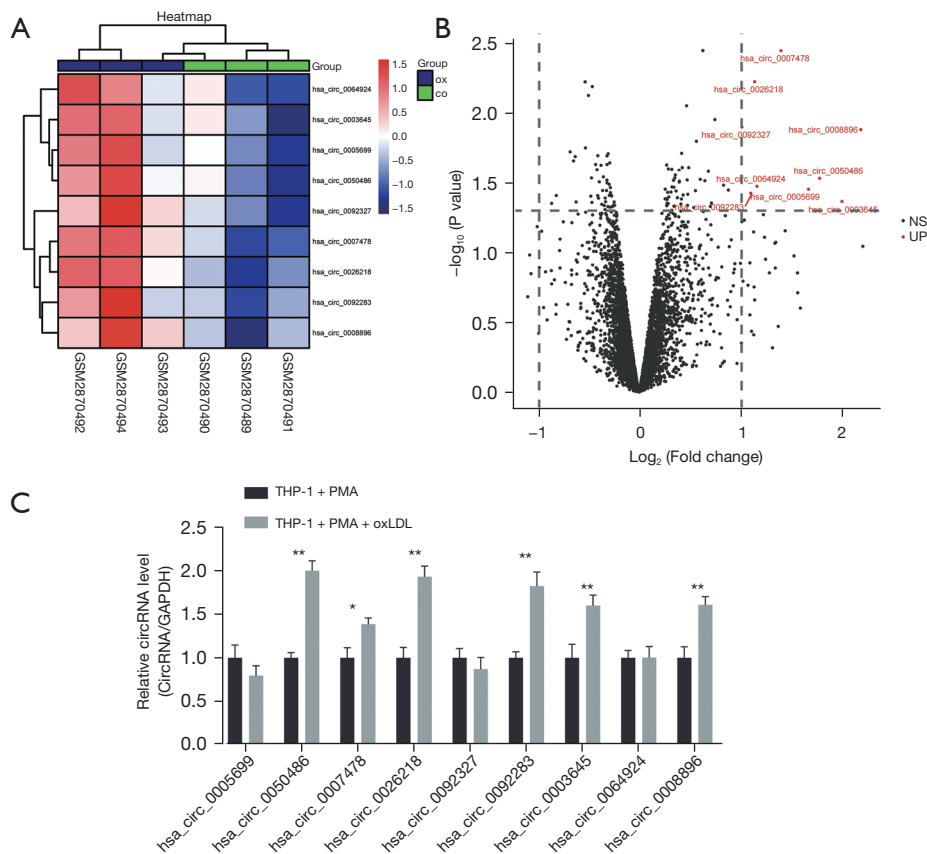


Figure 1 Identification of DECs in the THP-1 + PMA + oxLDL group compared with the control group. (A) The heatmap showing the significant DECs. Ox represents oxLDL treated group; co represents control group. (B) The red section of the volcano map represents upregulated circRNAs. NS represents no significant; UP represents upregulated. (C) A qRT-PCR assay was used to verify the DECs expression level in the THP-1 + PMA group and the THP-1 + PMA + oxLDL group. *, $P < 0.05$ and **, $P < 0.01$. DECs, differentially expressed circRNAs; PMA, phorbol 12-myristate 13-acetate; oxLDL, oxidized low-density lipoprotein; qRT-PCR, quantitative real-time reverse transcription polymerase chain reaction.

145, and *miR-182* (Figure 3B). The relative luciferase activity was significantly decreased in the model cells co-transfected with WT *circ_0050486*, and *miR-145* mimics or *miR-1270* mimics compared with NC; while the model cells co-transfected with MUT-*circ_0050486* and *miR-145* mimics or *miR-1270* mimics reversed the luciferase activity (Figure 3C). These results suggested that *miR-145* and *miR-1270* were target genes of *circ_0050486*.

Previous study has reported that *miR-145* promotes chronic inflammation by regulating multiple pathways in AS (19). Therefore, we chose *miR-1270* to further explore inflammation and apoptosis in the THP-1 + PMA + oxLDL cell model. IL-6 and TNF- α concentrations were detected using ELISA, and the results showed that upregulated *miR-1270* significantly inhibited IL-6 and TNF- α levels in

the model compared with NC (Figure 3D). Furthermore, cell apoptosis was detected with a flow cytometry assay, and results showed that upregulated *miR-1270* suppressed the apoptotic rates (Figure 3E). Together, these results suggested that knockdown of *circ_0050486* repressed the inflammatory response and apoptosis by targeting *miR-1270* in oxLDL-induced THP-1 macrophages.

Functional enrichment analysis of *miR-145* and *miR-1270* target genes

It has been reported that miRNAs regulate the development of AS by targeting the 3'UTR of the target genes. To further explore how the targeted miRNAs of *circ_0050486* regulated inflammation and apoptosis, we used the

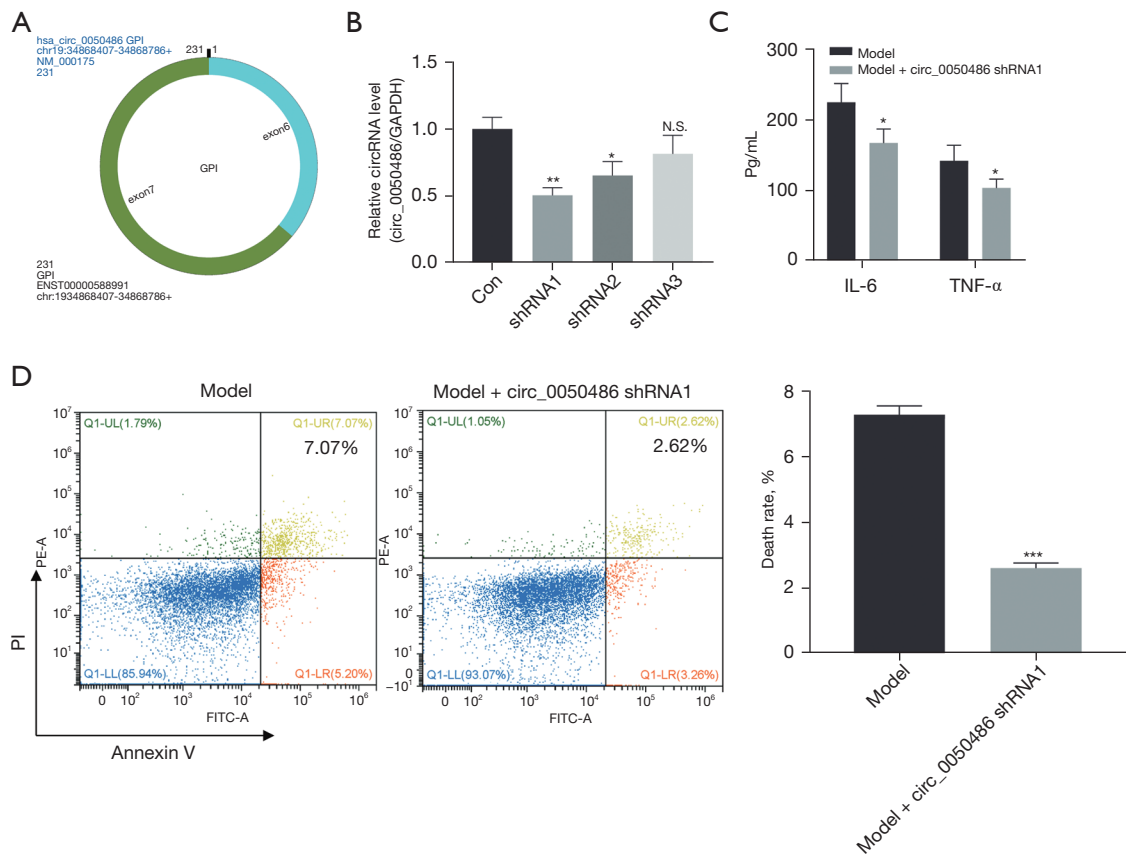


Figure 2 The effect of *circ_0050486* on inflammation and apoptosis in oxLDL-treated THP-1 macrophages. (A) The sequence characteristics of *circ_0050486*. (B) The relative expression level of *circ_0050486* measured by qRT-PCR assay in the model cells after shRNA transfection. NS represents no significant. (C) ELISA results detect the concentration of IL-6 and TNF- α . (D) Flow cytometry assay detects cell apoptosis. The column date represents the death rate%. *, $P < 0.05$, **, $P < 0.01$, ***, $P < 0.001$. oxLDL, oxidized low-density lipoprotein; qRT-PCR, quantitative real-time reverse transcription polymerase chain reaction; ELISA, enzyme-linked immunosorbent assay.

miRwalk, Targetscan, and miRDB databases to predict the target genes of *miR-145* and *miR-1270*. The functional enrichment analysis of *miR-145* and *miR-1270* targeted genes was established using Cytoscape software. As shown in *Figure 4A,4B*, the 56 target genes of *miR-145* were enriched in 19 functional pathways, and the 27 target genes of *miR-1270* were enriched in 21 functional pathways. Interestingly, these genes were enriched in immune response, embryonic hemopoiesis, monocyte chemotaxis, and T cell differentiation. A Venn diagram showed that 27 common target genes were found in the 446 target genes of *miR-145* and the 276 target genes of *miR-1270* (*Figure 4C*). The common target genes of *miR-145* and *miR-1270* are shown in *Figure 4D* and include NF1A, MMP16, and USP31. Furthermore, we found that these target genes were reported to regulate inflammation and apoptosis in

AS. Therefore, these results suggest that the target genes of *circ_0050486* targeting *miR-145* and *miR-1270* could be potential therapeutic targets of AS.

Discussion

AS is a major cause of cardiovascular disease and is associated with high morbidity and mortality worldwide (20). Moreover, clinical and experimental studies have revealed that aging and inflammation are factors associated with the increased incidence of atherosclerosis (21). The discovery of ncRNAs, including miRNAs, lncRNAs, and circRNAs, and their identification as key regulators in biological processes has made them a research focus in various diseases (22). CircRNAs have been explored in the diagnosis and treatment of various diseases via gene sequencing data

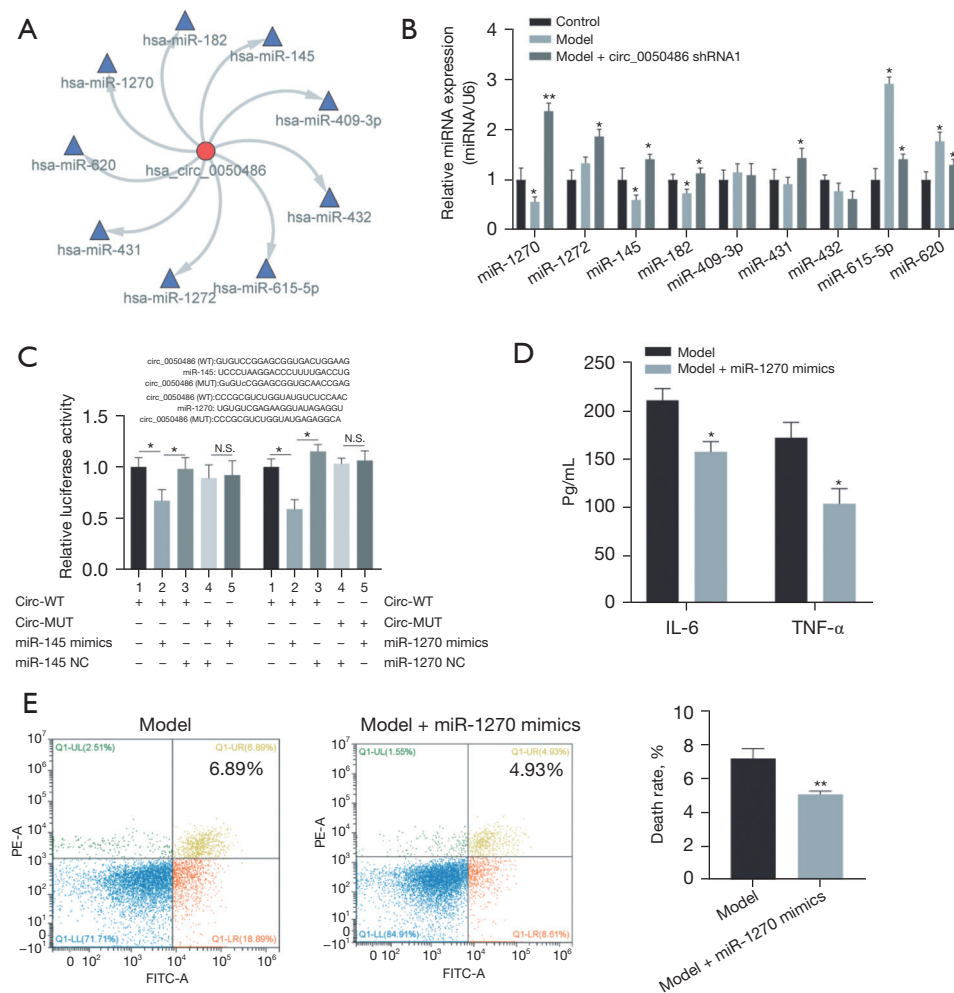


Figure 3 The *circ_0050486* targeted gene *miR-1270* inhibits inflammation and apoptosis in the model cells. (A) The potential target miRNAs for *circ_0050486* predicted by CircRNA Interactome. (B) The relative expression level of target miRNAs using qRT-PCR analysis. (C) The luciferase gene assay results analyze the luciferase activity in cells co-transfected with WT *circ_0050486* and *miR-145* mimics or *miR-1270* mimics. NS represents no significant. (D) The IL-6 and TNF- α concentrations detected by ELISA. (E) The apoptosis rates detected by flow cytometry assay. *, $P < 0.05$, **, $P < 0.01$. qRT-PCR, quantitative real-time reverse transcription polymerase chain reaction; ELISA, enzyme-linked immunosorbent assay; WT, wild type; MUT, mutant.

analysis and bioinformatics technologies (23). In this study, we analyzed microarray datasets to identify nine upregulated DECs in GSE107522. The qRT-PCR assay verified that the mRNA levels of *bas_circ_0050486*, *bas_circ_0007478*, *bas_circ_0026218*, *bas_circ_0092283*, *bas_circ_003645*, and *bas_circ_0008896* were markedly increased in the THP-1 + PMA + α LDL group compared with the THP-1 + PMA group. Of these, *has_circ_0050486* had the most significantly increased mRNA level compared with the THP-1 + PMA group. Next, we chose *bas_circ_0050486* to explore its function and molecular mechanism in the

THP-1 + PMA + α LDL group. Although one study has confirmed that *circ_0050486* can regulate MYD88 expression through competitively binding to *miR-182-5p* in α LDL-induced endothelial cell injury (6). As we all know, a single circRNA can bind and target multiple miRNAs to play different roles (24), and the pathogenesis of AS is characterized by multiple pathological processes (2,3).

Chronic inflammation plays a key role in AS progression (25,26). The inflammatory response not only predicts the risk of vascular events but also participates in the

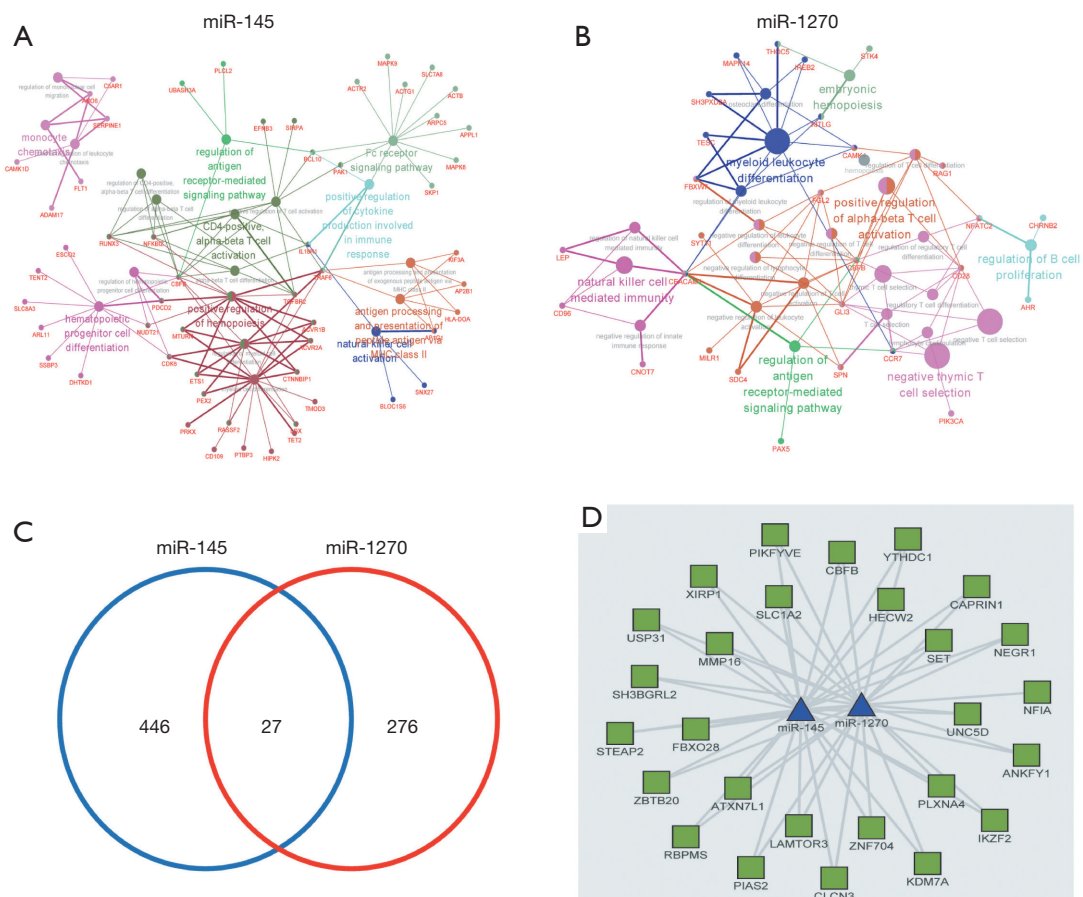


Figure 4 Functional enrichment analysis. (A,B) The target genes of *miR-145* (A) and *miR-1270* (B) using functional enrichment analysis. (C) The Venn diagram revealing the 27 common target genes of *miR-145* and *miR-1270*. (D) The construction of the common target genes network regulated by *miR-145* and *miR-1270*. Triangles indicate miRNAs and squares represent target mRNAs.

pathogenesis of AS-related diseases (27). Previous studies have suggested that biomarkers in the inflammation process have become the main index to evaluate atherosclerosis (28-30). Recent studies have found that circRNAs regulate inflammation in atherosclerosis (31,32). For example, circRNA RSF1 regulated oxLDL-treated vascular endothelial cell inflammation and apoptosis in AS by regulating the *miR-135b-5p/HDAC1* axis (31). However, the mechanisms for AS are not fully understood. Here, we investigated the effect of *circ_0050486* on inflammation and apoptosis in AS, which revealed knockdown of *circ_0050486* inhibited IL-6 and TNF- α concentrations and the apoptosis rates in oxLDL-induced THP-1 macrophages.

To fully understand the potential mechanisms of *circ_0050486*-targeted miRNA in AS, we explored *circ_0050486*-miRNA interaction data to construct a *circ_0050486*-miRNA network. We found that nine miRNAs

were targeted genes of *circ_0050486* and identified that *circ_0050486* significantly decreased the level of *miR-145* and *miR-1270* in oxLDL-induced THP-1 macrophages. Recently, miRNA sequencing and bioinformatics analysis demonstrated that *miR-145* was associated with AS (33,34). It was reported that *miR-145* suppressed the inflammatory reaction in AS cells and mice by activating NF- κ B signaling (35). A previous study also found that *miR-145* inhibited cell proliferation and improved metabolic inflammation in type 2 diabetes and AS by targeting OPG and KLF5 (19). There have been no previous reports on the role of *miR-1270* in AS. Our study found that *miR-1270* significantly inhibited IL-6 and TNF- α concentrations and apoptosis rates in the model cells compared with the NC cells. These results suggested that knockdown of *circ_0050486* repressed inflammation and apoptosis by targeting *miR-1270* in oxLDL-induced THP-1 macrophages.

Our functional enrichment analysis showed that the target genes of *miR-145* and *miR-1270* were enriched in the biological processes of immune response, regulation of antigen receptor-mediated signaling pathway, embryonic hemopoiesis, monocyte chemotaxis, and T cell differentiation. It has been reported that monocytes and macrophages play essential roles in atherosclerotic lesions (36,37). A previous study has suggested the potential role of monocyte chemotaxis in the development of cardiovascular diseases (38). In this study, the common target genes of *miR-145* and *miR-1270*, including NF1A, were predicted using the miRwalk, Targetscan, and miRDB databases. It has previously been reported that NF1A overexpression suppresses pro-inflammatory cytokines and can improve AS progression (39). Another study reported that the upregulation of NF1A decreased the formation of atherosclerotic plaques in plasma by suppressing pro-inflammatory factor levels (40). Additionally, Chen *et al.* found that upregulated *MALAT1* improved AS progression by regulating the *miR-155-5p/NF1A* axis (41). In this study, *circ_0050486* inhibited inflammation and apoptosis by targeting the *miR-1270/NF1A* axis, although this remains to be further verified. Our findings suggested that *circ_0050486* may be a potential therapeutic target for atherosclerosis. However, there are some problems and challenges that need to be overcome in the clinical application of circRNAs. At present, specific circRNAs as biomarkers or therapeutic targets are in their infancy, whether circRNAs are highly specific for diseases is unknown, and most of the studies are basic research rather than clinical application research.

Conclusions

Our study demonstrated that the underlying mechanism and function of *circ_0050486* is in regulating inflammation and apoptosis by targeting *miR-1270* in oxLDL-induced THP-1 macrophages. Knockdown of *circ_0050486* is regarded as a potential therapeutic target for reducing the inflammatory reaction in atherosclerosis pathology. Our results suggested that *circ_0050486* may play an essential regulatory role in AS by targeting *miR-1270*, providing further evidence for AS research. The specific molecular regulatory mechanism will need to be elucidated in future research.

Acknowledgments

Funding: This work was supported by the Inner Mongolia Natural Science Foundation (No. 2018LH08046); the

Doctor Starting Fund of the Affiliated Hospital of Inner Mongolia Medical University (No. NYFYBS2018, to Feng Jin); the National Natural Science Foundation of China (No. 81860558); the Inner Mongolia Medical University Affiliated Hospital Doctor Fund Project (No. NYFYBS2018, to Kai Wang); the General project of the Inner Mongolia Natural Science Foundation (No. 2018LH08040); and the Inner Mongolia Medical University Science and Technology Million (Joint) Project [No. YKD2017KJBW (LH) 003].

Footnote

Reporting Checklist: The authors have completed the MDAR reporting checklist. Available at <https://atm.amegroups.com/article/view/10.21037/atm-22-3745/rc>

Data Sharing Statement: Available at <https://atm.amegroups.com/article/view/10.21037/atm-22-3745/dss>

Conflicts of Interest: All authors have completed the ICMJE uniform disclosure form (available at <https://atm.amegroups.com/article/view/10.21037/atm-22-3745/coif>). All authors report that this work was supported by the Inner Mongolia Natural Science Foundation (No. 2018LH08046), the National Natural Science Foundation of China (No. 81860558), the General project of the Inner Mongolia Natural Science Foundation (No. 2018LH08040), and the Inner Mongolia Medical University Science and Technology Million (Joint) Project [No. YKD2017KJBW (LH) 003]. KW reports that this work was supported by the Inner Mongolia Medical University Affiliated Hospital Doctor Fund Project (No. NYFYBS2018). FJ reports that this work was supported by the Doctor Starting Fund of the Affiliated Hospital of Inner Mongolia Medical University (No. NYFYBS2018). The authors have no other conflicts of interest to declare.

Ethical Statement: The authors are accountable for all aspects of the work in ensuring that questions related to the accuracy or integrity of any part of the work are appropriately investigated and resolved. The study was conducted in accordance with the Declaration of Helsinki (as revised in 2013).

Open Access Statement: This is an Open Access article distributed in accordance with the Creative Commons Attribution-NonCommercial-NoDerivs 4.0 International License (CC BY-NC-ND 4.0), which permits the non-

commercial replication and distribution of the article with the strict proviso that no changes or edits are made and the original work is properly cited (including links to both the formal publication through the relevant DOI and the license). See: <https://creativecommons.org/licenses/by-nc-nd/4.0/>.

References

- Libby P. The changing landscape of atherosclerosis. *Nature* 2021;592:524-33.
- Shan R, Liu N, Yan Y, et al. Apoptosis, autophagy and atherosclerosis: Relationships and the role of Hsp27. *Pharmacol Res* 2021;166:105169.
- Knutson AK, Williams AL, Boisvert WA, et al. HIF in the heart: development, metabolism, ischemia, and atherosclerosis. *J Clin Invest* 2021;131:e137557.
- Soehnlein O, Libby P. Targeting inflammation in atherosclerosis - from experimental insights to the clinic. *Nat Rev Drug Discov* 2021;20:589-610.
- He X, Fan X, Bai B, et al. Pyroptosis is a critical immune-inflammatory response involved in atherosclerosis. *Pharmacol Res* 2021;165:105447.
- Zhang P, Wang W, Li M. Role and mechanism of circular RNA *circ_0050486* in regulating oxidized low-density lipoprotein-induced injury in endothelial cells. *Clin Hemorheol Microcirc* 2022. [Epub ahead of print]. doi: 10.3233/CH-211259.
- Liang Y, Liu N, Yang L, et al. A Brief Review of circRNA Biogenesis, Detection, and Function. *Curr Genomics* 2021;22:485-95.
- Wong LM, Phoon LQ, Wei LK. Epigenetics Modifications in Large-Artery Atherosclerosis: A Systematic Review. *J Stroke Cerebrovasc Dis* 2021;30:106033.
- Zheng D, Huo M, Li B, et al. The Role of Exosomes and Exosomal MicroRNA in Cardiovascular Disease. *Front Cell Dev Biol* 2020;8:616161.
- Tang X, Ren H, Guo M, et al. Review on circular RNAs and new insights into their roles in cancer. *Comput Struct Biotechnol J* 2021;19:910-28.
- Zheng S, Zhang X, Odame E, et al. CircRNA-Protein Interactions in Muscle Development and Diseases. *Int J Mol Sci* 2021;22:3262.
- Liu Y, Yang Y, Wang Z, et al. Insights into the regulatory role of circRNA in angiogenesis and clinical implications. *Atherosclerosis* 2020;298:14-26.
- Altesha MA, Ni T, Khan A, et al. Circular RNA in cardiovascular disease. *J Cell Physiol* 2019;234:5588-600.
- Zeng Z, Xia L, Fan S, et al. Circular RNA *CircMAP3K5* Acts as a MicroRNA-22-3p Sponge to Promote Resolution of Intimal Hyperplasia Via TET2-Mediated Smooth Muscle Cell Differentiation. *Circulation* 2021;143:354-71.
- Dudekula DB, Panda AC, Grammatikakis I, et al. CircInteractome: A web tool for exploring circular RNAs and their interacting proteins and microRNAs. *RNA Biol* 2016;13:34-42.
- Dweep H, Gretz N, Sticht C. miRWalk database for miRNA-target interactions. *Methods Mol Biol* 2014;1182:289-305.
- Chen Y, Wang X. miRDB: an online database for prediction of functional microRNA targets. *Nucleic Acids Res* 2020;48:D127-31.
- Bindea G, Mlecnik B, Hackl H, et al. ClueGO: a Cytoscape plug-in to decipher functionally grouped gene ontology and pathway annotation networks. *Bioinformatics* 2009;25:1091-3.
- He M, Wu N, Leong MC, et al. miR-145 improves metabolic inflammatory disease through multiple pathways. *J Mol Cell Biol* 2020;12:152-62.
- Valanti EK, Dalakoura-Karagkouni K, Siasos G, et al. Advances in biological therapies for dyslipidemias and atherosclerosis. *Metabolism* 2021;116:154461.
- Ruiz-León AM, Lapuente M, Estruch R, et al. Clinical Advances in Immunonutrition and Atherosclerosis: A Review. *Front Immunol* 2019;10:837.
- Chen W, Guo S, Li X, et al. The regulated profile of noncoding RNAs associated with inflammation by tanshinone IIA on atherosclerosis. *J Leukoc Biol* 2020;108:243-52.
- Fasolo F, Di Gregoli K, Maegdefessel L, et al. Non-coding RNAs in cardiovascular cell biology and atherosclerosis. *Cardiovasc Res* 2019;115:1732-56.
- Yu CY, Kuo HC. The emerging roles and functions of circular RNAs and their generation. *J Biomed Sci* 2019;26:29.
- Poznyak A, Grechko AV, Poggio P, et al. The Diabetes Mellitus-Atherosclerosis Connection: The Role of Lipid and Glucose Metabolism and Chronic Inflammation. *Int J Mol Sci* 2020;21:1835.
- Ley K. Inflammation and Atherosclerosis. *Cells* 2021;10:1197.
- Pedro-Botet J, Climent E, Benaiges D. Atherosclerosis and inflammation. New therapeutic approaches. *Med Clin (Barc)* 2020;155:256-62.
- Groenen AG, Halmos B, Tall AR, et al. Cholesterol efflux pathways, inflammation, and atherosclerosis. *Crit Rev Biochem Mol Biol* 2021;56:426-39.

29. Zhang H, Ge S, Ni B, et al. Augmenting ATG14 alleviates atherosclerosis and inhibits inflammation via promotion of autophagosome-lysosome fusion in macrophages. *Autophagy* 2021;17:4218-30.
30. Zhu Y, Xian X, Wang Z, et al. Research Progress on the Relationship between Atherosclerosis and Inflammation. *Biomolecules* 2018;8:80.
31. Zhang X, Lu J, Zhang Q, et al. CircRNA RSF1 regulated ox-LDL induced vascular endothelial cells proliferation, apoptosis and inflammation through modulating miR-135b-5p/HDAC1 axis in atherosclerosis. *Biol Res* 2021;54:11.
32. Li D, Jin W, Sun L, et al. Circ_0065149 Alleviates Oxidized Low-Density Lipoprotein-Induced Apoptosis and Inflammation in Atherosclerosis by Targeting miR-330-5p. *Front Genet* 2021;12:590633.
33. Yang W, Yin R, Zhu X, et al. Mesenchymal stem-cell-derived exosomal miR-145 inhibits atherosclerosis by targeting JAM-A. *Mol Ther Nucleic Acids* 2021;23:119-31.
34. Lv Y, Yi Y, Jia S, et al. The miR-145 rs353291 C allele increases susceptibility to atherosclerosis. *Front Biosci (Landmark Ed)* 2020;25:577-92.
35. Li S, Sun W, Zheng H, et al. MicroRNA-145 accelerates the inflammatory reaction through activation of NF- κ B signaling in atherosclerosis cells and mice. *Biomed Pharmacother* 2018;103:851-7.
36. Feng X, Chen W, Ni X, et al. Metformin, Macrophage Dysfunction and Atherosclerosis. *Front Immunol* 2021;12:682853.
37. Jin L, Deng Z, Bai Y, et al. Functions of Monocytes and Macrophages and the Associated Effective Molecules and Mechanisms at the Early Stage of Atherosclerosis. *Acta Cardiol Sin* 2021;37:522-33.
38. Kassiteridi C, Cole JE, Griseri T, et al. CD200 Limits Monopoiesis and Monocyte Recruitment in Atherosclerosis. *Circ Res* 2021;129:280-95.
39. Zhao JJ, Hu YW, Huang C, et al. Dihydrocapsaicin suppresses proinflammatory cytokines expression by enhancing nuclear factor IA in a NF- κ B-dependent manner. *Arch Biochem Biophys* 2016;604:27-35.
40. Hu YW, Zhao JY, Li SF, et al. RP5-833A20.1/miR-382-5p/NFIA-dependent signal transduction pathway contributes to the regulation of cholesterol homeostasis and inflammatory reaction. *Arterioscler Thromb Vasc Biol* 2015;35:87-101.
41. Chen L, Hu L, Zhu X, et al. MALAT1 overexpression attenuates AS by inhibiting ox-LDL-stimulated dendritic cell maturation via miR-155-5p/NFIA axis. *Cell Cycle* 2020;19:2472-85.

Cite this article as: Wang K, Bai X, Mei L, Miao Y, Jin F. *CircRNA_0050486* promotes cell apoptosis and inflammation by targeting *miR-1270* in atherosclerosis. *Ann Transl Med* 2022;10(16):905. doi: 10.21037/atm-22-3745